Non-linear Control Applied to a 3D Printed Hand

Sofiane Ibrahim Benchabane[1(✉)], Nadia Saadia[1], and Amar Ramdane-Cherif[2]

[1] University of Science and Technology Houari Boumediene, Bab Ezzouar, Algeria
[2] Versailles Saint-Quentin-en-Yvelines University, Versailles, France

Abstract. The dynamics of a prosthesis is an important parameter to consider in order to allow efficient use. In fact, the prosthesis should perform the desired task with enough precision under a controlled kinematics. To this aim, it is necessary to set up a control law which guarantees the operating of the structure according to a pre-established specification. A prosthesis like any mechatronic structure is a complex and dynamic system, based on parameters which can evolve as a function of interactions, physical conditions or time, for this it is necessary to use a robust control algorithm to address this issue. In this work we present a sliding mode control algorithm applied to an anthropomorphic prosthesis printed in 3D at the LRPE/LISV laboratories. The control structure used enables to overcome the modelling uncertainties and parametric variations of the mechatronic system such as the coefficients of friction in the joints and the coefficient of elasticity of cable-pull.

Keywords: Prosthetic control · Sliding mode control · Non-linear control

1 Adaptive Control

A linear system is a system whose output (s) are a linear combination of its input (s), in other words the system is represented by a linear transfer function where when the input of the system varies, the output varies similarly. The control of such a system is a task which consists in determining a control law constraining the response of the system to a desired dynamic. In order to synthesize this control law, it is generally sufficient to study the response of the system to a predefined set point (a step for example) thanks to the system's linearity its behaviour will be similar for any finite input (invariant causal system).

In the case where the system considered is linear but variable, that is to say that its parameters are not constant over time (aging, parameters sensitive to temperature, humidity, mechanical stress, etc.), the control law can turn out to be 'obsolete' and no longer guarantees the control of the system in all circumstances.

Several approaches can be implemented in the context of variable structure control such as: neural networks [1–8], fuzzy logic [9–11], the neurofuzzy approach [12–16], sliding mode control [17–21].

S. Paiva et al. (Eds.): SmartCity360° 2020, LNICST 372, pp. 140–155, 2021.
https://doi.org/10.1007/978-3-030-76063-2_11

The sliding mode control is a very popular strategy for control of nonlinear uncertain systems, with a very large frame of applications fields [22, 23]. The main drawback of the sliding mode control, the well-known chattering phenomenon [24, 25] is important and could damage actuators and systems. A first way to reduce the chattering is the use of a boundary layer: in this case, many approaches have proposed adequate controller gains tuning [26]. A second way to decrease the chattering phenomenon is the use of higher order sliding mode controller [27–30]. However, in both these control approaches, knowledge of uncertainties bound is required.

The Sliding Mode Control (SMC) is a command which is not sensitive to parametric variations as well as to modelling uncertainties, the approach also brings good results as regards resistance to disturbances.

The implementation of this method is relatively simple and does not affect the performance of the system in terms of response time. The SMC ensures the stability of the system by maintaining its state on the hyperplane S = 0, as illustrated in Fig. 1.

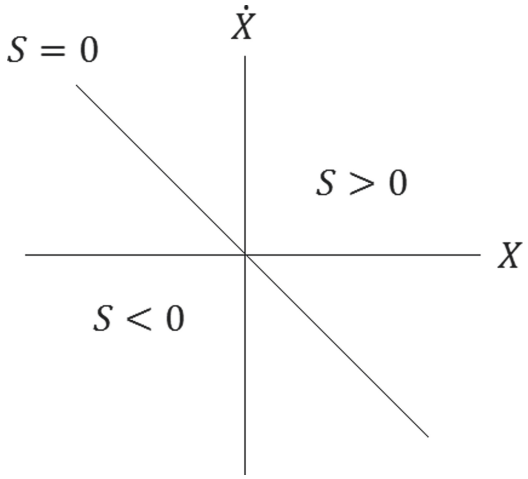

Fig. 1. Hyperplane S in the state space, when the system is on the right S = 0 it is in sliding mode

In the state space, we can define the line $S = \dot{X} + \sigma X, \sigma > 0$ where X is a state vector.

$$S = 0 \rightarrow \dot{X} = -\sigma X \rightarrow x(t) = Ce^{-\sigma t} \tag{1}$$

The Eq. (1) allows to affirm that the variable of state of the system tends towards 0 in a finite time, in other words the system will bring a finished response to a finished entry when $S = 0$ (system in sliding mode). Therefore, in order to ensure the stability of the system it is sufficient to maintain the system on the hyperplane $S = 0$. However, it is also necessary that the control law makes it possible to ensure the accuracy of the system by cancelling at the same time the system error e. By simply choosing to set $X = e$ when the system will be in sliding mode, we will therefore obtain that $e \rightarrow 0$, ensuring the precision and stability of the system. The control will therefore consist in

evaluating S and acting on the setpoint of the system in order to bring it back on the hyperplane.

2 The Studied System

The studied system includes an EMG interface [31] who provides instructions for function enabling/disabling, i.e. determines which appropriate function to activate. Once this instruction is generated the system should execute it properly by driving it to a precise dynamic, as illustrated in Fig. 2.

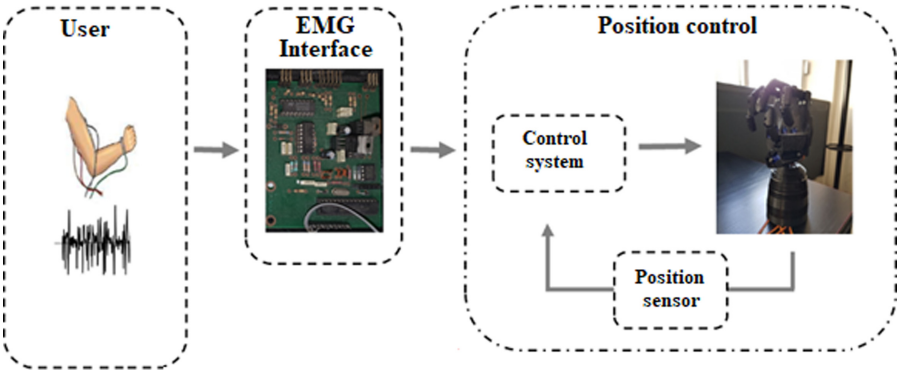

Fig. 2. Diagram of the different system's modules.

Beforehand, it is necessary to define the different components of the system as well as the specifications imposed on it. The system developed consists of the elements described below.

2.1 Setpoint Generator

In our system while the EMG module delivers a signal, the system remains operating (flexion or extension of the finger is held). To this end, the setpoint generator increments the desired angle every 200 ms while the activation signal at its input is present. Indeed, we require that a complete flexion or extension is performed in 20 steps of 4.5° each and in 4 s.

2.2 System to Control

The system to be controlled consists of the actuator (servomotor) and the prosthesis, an angular position sensor is incorporated on the servomotor lifter, which will be used to measure the angle provided by the actuator at the input of the mechanical device.

The setpoint generator will therefore indicate a desired angle to be reached (from the signal delivered by the EMG module), then the system (actuator, prosthesis) will have to satisfy this constraint. Figure 3 below illustrates the system:

Fig. 3. Global diagram of the system to be controlled (servo + prosthesis)

The actuator is controlled by Pulse Width Modulation (PWM), namely is necessary to code the angle requested from the actuator by varying the duty cycle of the signal applied to it. For this reason, our system therefore incorporates a desired angle encoder, which will convert the setpoint angle into a signal "understandable" by the servomotor (modulated in pulse width).

2.2.1 The Desired Angle Encoder

The role of this module is to match the desired angle φ_d to a pulse width to be sent to the servomotor. In order to determine the pulse width which corresponds to a given angle, we apply a simple rule of three from the technical data sheet of the actuator:

$$180° \rightarrow 1\ ms\ width$$

$$angle° \rightarrow t\ ms\ width$$

i.e.

$$t = \frac{angle}{180} 10^{-3} s \tag{2}$$

2.2.2 The Servomotor

The servomotor used in our system is the (SG90), producing a torque $T_u = 1.63$ Kg.cm.cm and a constant angular speed $\omega_{mot} = 600°/s$, under a supply voltage of 5 V. A servo motor is actually a DC motor with gears and a position control loop. In our approach, we consider the servomotor as the assembly of the following two modules:

A Pulse Width Converter: which corresponds to a variation in pulse width α of a DC motor operating time. Indeed, given that the motor rotates at a constant speed w_{mot} with a constant torque Tu, the position of the motor depends on the activation time of the latter. It is therefore necessary to establish the relationship between α is the operating time of the DC motor $t(\alpha)$ integrated in the servomotor.

A DC Motor: which delivers the position corresponding to the supply duration defined by the pulse width α. The engine is characterized by the electromechanical equations given below.

Figure 4 shows the SG90 and its various components:

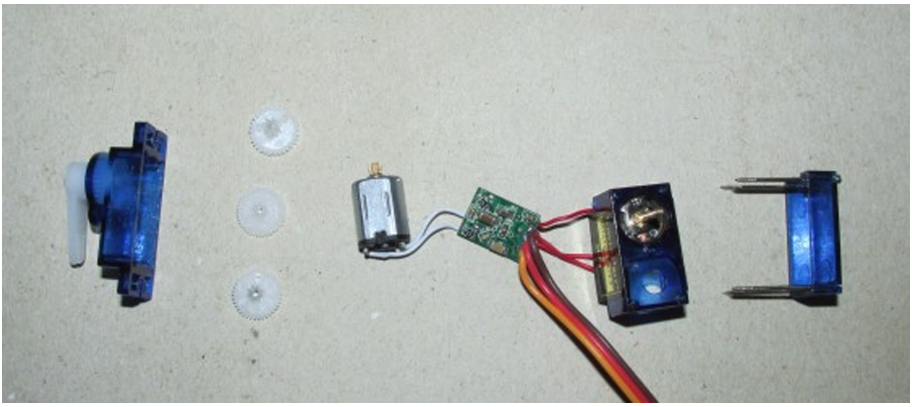

Fig. 4. The various constituents of SG90.

As shown in the Fig. 4, the servomotor is made up of: on the left the lifter and the reduction system, in the centre the direct current motor and its servo circuit, on the right the servomotor cover.

2.2.3 The Prosthetic Finger

The mechanical system (prosthesis) is the decoupled set of 5 fingers where each finger is an independent system, the control of our prosthesis therefore requires the control of each finger independently of the others.

The finger consists of 3 articulated phalanges, the angle of rotation of each joint is dependent on the angle of rotation of the motor as given below.

An angular position sensor linked to the servomotor lifter, delivers a voltage proportional to the measured angle of rotation, the sensor is positioned on the motor, and the flexion/extension angle of the finger and deduced from the relation $\varphi = f(\theta)$.

3 Specifications

The system developed is governed by specifications that we impose, as described in the following:

1. While the corresponding EMG function is active, the actuator is activated, and the finger is in motion.
2. 2. φ_r is the angle of flexion/extension of the finger identified from the end of the phalanx 3 to the carpus, $\varphi_r \in [0° - 180°]$.
3. A finger performs a complete flexion or extension in 4s.
4. A flexion or extension is completed in 20 steps of 4.5° each of the servomotor lifter (θ_M).
5. The movement of a finger is characterized by a constant dynamic (constant motor torque, constant motor angular speed).

4 Synoptic Diagram

In the dynamics that we impose on our system, a function remains activated while the EMG signal corresponding to its activation is present. This function is provided by a block which will be called the setpoint generator, which will deliver the duty cycle necessary to animate the structure according to the presence of the EMG signal.

Let T given in Eq. (3) be the transfer function of our open loop system, the block diagram according to Fig. 5 represents the open loop system.

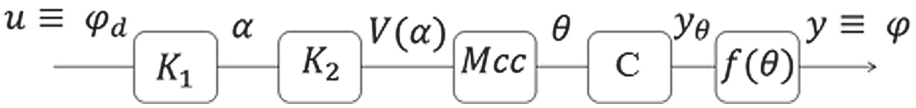

Fig. 5. Synoptic diagram of the sound system, including all the constituent segments of the system to be controlled

From the synoptic diagram we express the transfer function of the system in open loop:

$$T = K_1 K_2 MCCf(\theta)C \tag{3}$$

5 Transfer Functions

5.1 The Desired Angle Encoder (K_1)

Convert the input setpoint to PWM (α), α is calculated by a simple rule of three, indeed, a variation of the pulse width of 1 ms corresponds to an angle of 180° where the angle φ_d corresponds to a variation of pulse width of $\varphi_d \frac{0.001}{180}$.

i.e.

$$\alpha = \varphi_d 5.56 \; then \; K_1 = 5.5610^{-5} \tag{4}$$

5.2 Pulse Width Converter (K_2)

The pulse width converter translates α into voltage (supply time) at the input of the DC motor as illustrated by Eq. (5)

$$V_s = t(\alpha).E \tag{5}$$

Figure 6 illustrates the evolution of $t(\alpha)$.

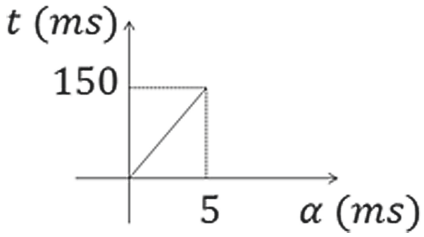

Fig. 6. The relation between α and the activation time required for the motor to reach the desired angle, knowing w_{mot}

From the Fig. 6 we have:

$$t(\alpha) = 30\alpha \tag{6}$$

Therefore:

$$K_2 = 30E \tag{7}$$

5.3 The DC Motor (MCC)

The DC motor is characterized by the following electromechanical equations:

$$\begin{cases} U = Ri + L\frac{di}{dt} + k\frac{d\theta}{dt} \\ J\frac{d^2\theta}{dt^2} = Tu = ki \end{cases} \tag{8}$$

Given:

L, R, k, J the electromechanical parameters of the motor. We set L → 0, from (8) we obtain:

$$U(p) = \frac{RJ}{k}p^2\theta(p) + kp\theta(p) \rightarrow \frac{\theta(p)}{U(p)} = \frac{k}{k^2p + RJp^2} \tag{9}$$

The electrical resistance of the motor is determined experimentally, R = 19 Ω.

5.4 The Finger ($f(\theta)$)

The prosthesis is considered as a decouplable system or each finger can be ordered separately. A finger is a system with 3 pivot joints, as shown in Fig. 7.

From Fig. 7 we can summarize:

$$\begin{cases} x = x_1 + x_2 + x_3 \rightarrow x = L\sum_{i=1}^{3}\sin(\mathrm{i}\theta) \\ y = y_1 + y_2 + y_3 \rightarrow y = L\sum_{i=1}^{3}\cos(\mathrm{i}\theta) \end{cases} \rightarrow \tan\varphi = \frac{\sum_{i=1}^{3}\sin(i\theta)}{\sum_{i=1}^{3}\cos(i\theta)}$$

Therefore:

$$\varphi = Arctg\left(\frac{\sum_{i=1}^{3}\sin(i\theta)}{\sum_{i=1}^{3}\cos(i\theta)}\right) \tag{10}$$

Figure 8 shows the plot of the angle φ as a function of the angle θ.

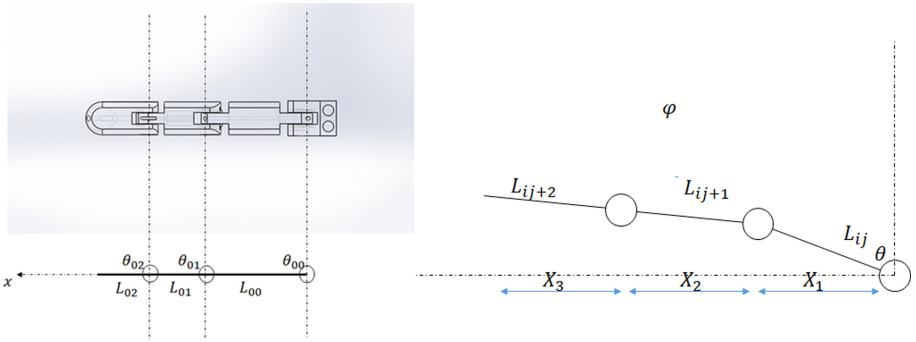

Fig. 7. Diagram illustrating $\varphi = f(\theta)$.

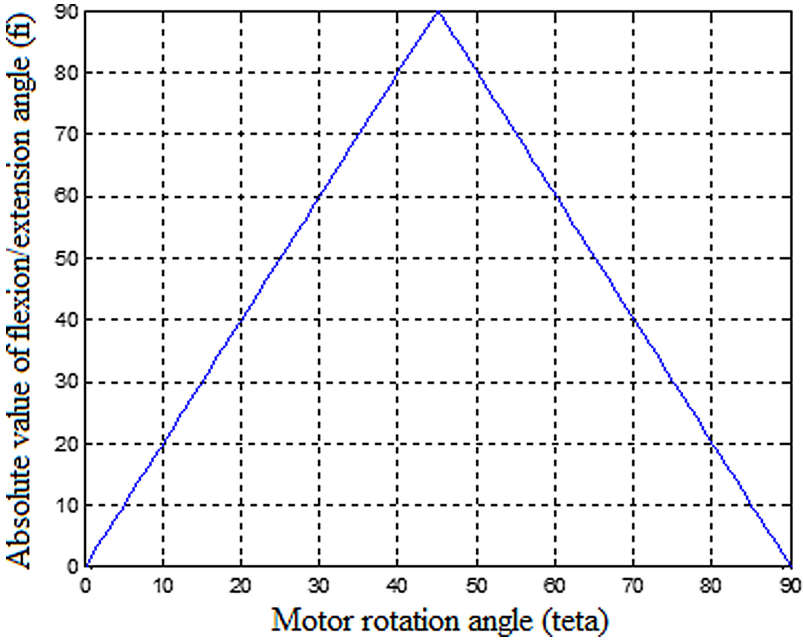

Fig. 8. Plot on Matlab of the relation $\varphi = f(\theta)$.

The negative slope part represents φ in the 3rd quadrant of the trigonometric circle (3π/2). Figure 8 shows the relationship between the bending angle of the finger and the angle of rotation of the motor, when the motor rotates 90° the finger makes an angle of 180°. From the figure we deduce the Eq. (11)

$$\varphi \approx 2\theta \tag{11}$$

The relation between φ and θ is approximated by a slope equal to 2.

5.5 Angular Position Sensor (*C*)

The angular position sensor allows us to measure the rotation angle of the motor, thanks to the Eq. (11) it is therefore possible to go back to the bending angle of the finger (φ). The sensor is characterized by the Eq. (12), linking its input to its output.

$$V_c = g(\theta) \rightarrow V_c = c.\theta \tag{12}$$

c is the sensitivity of the sensor, the voltage delivered by the angular sensor is proportional to the angle of rotation measured. The sensor used in our application is a horizontal rotary potentiometer (1 kΩ, 20% tolerance), the calculation of the sensitivity goes through the development of the sensor conditioning circuit.

We deduce the angle of rotation from the output voltage delivered by the conditioning circuit, this is directly related to the value of the resistance of the potentiometer, which in turn depends on the position of the axis of l "adjustable (coupled to the axis of rotation of the servomotor). Conditioning requires a constant current source, in fact, so that the output voltage is proportional to the angle of rotation (therefore the value of the resistance) it is necessary that the current passing through the variable resistance is constant.

$$C = 0.13 \mp 20\% \tag{13}$$

5.6 Open Loop and Closed Loop Transfer Functions

In open loop the system is the cascading of the different modules which constitute it (Fig. 5) so we get:

$$T = \frac{K_1 K_2 2ck}{k^2 p + RJp^2} = \frac{\acute{K}}{RJp^2 + k^2 p} \tag{14}$$

The knowledge of the transfer function of the system in opened loop makes it possible to ensure an order insofar as it is possible to find the necessary setpoint, to be applied to the system in order to obtain the desired output. However, in this configuration it is not possible to be sure that the system output corresponds to the desired one, moreover if the output is affected by a disturbance no action can compensate the setpoint accordingly. It is then necessary to ensure the servo-control of the system by reporting its output to the set point (command in closed loop). The following block diagram (Fig. 9) represents the closed loop system:

The transfer function of the system when the output is brought back to the input is of the second order form and is given in the Eq. (14)

$$F = \frac{T}{1 + T}$$

$$F = \frac{\acute{K}}{RJp^2 + k^2 p + \acute{K}}$$

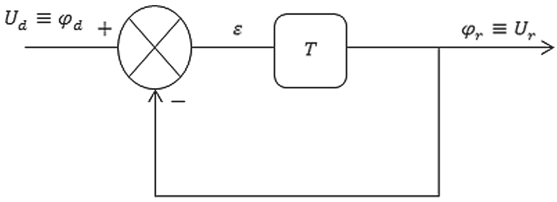

Fig. 9. Block diagram of the closed loop system

$$F = \frac{1}{\frac{RJ}{K'}p^2 + \frac{k^2}{K'}p + 1}$$

$$F = \frac{1}{9103.45p^2 + 3.096p + 1} \tag{15}$$

The system consists of modules whose parameters are subject to variation over time. Indeed, the parameters of the electric motor such as the armature resistance R, the flux constant k can change. The relation f (θ) is also sensitive to variations, this has been graphically approximated and can change over time, since it is strongly correlated to the fictions of the joints, to the stiffness of the return cable which can also evolve over time. The sensitivity of the sensor can also be affected by modelling uncertainty.

It is therefore wise to consider a robust control approach that is not very sensitive to parametric variation as well as to modelling errors. For this, we are oriented on an adaptive or variable structure control approach.

6 State-Space Representation of the System

We pass from the transfer function in closed loop of our system to its representation in the state space as follows:

From (14)

$$\frac{Y(p)}{U(p)} \rightarrow U(p) = c_1 p^2 Y(p) + c_0 p Y(p) + Y(p); c_1 = \frac{RJ}{K'}, c_0 = \frac{k^2}{K'} \tag{16}$$

$$(16) \rightarrow^{TL^{-1}} u(t) = c_1 \ddot{y}(t) + c_0 \dot{y}(t) + y(t)$$

By putting:

$$\begin{cases} x_1(t) = y(t) \\ x_2(t) = \dot{y}(t) \\ \begin{cases} \dot{x}_1(t) = \dot{y}(p) \\ \dot{x}_2(t) = \ddot{y}(p) \end{cases} \end{cases} \tag{18}$$

The transition to the canonical form gives us:

$$\begin{cases} \begin{pmatrix} \dot{x}_1(t) \\ \dot{x}_2(t) \end{pmatrix} = \begin{pmatrix} 0 & 1 \\ -\frac{1}{c_1} & -\frac{c_0}{c_1} \end{pmatrix} \begin{pmatrix} x_1(t) \\ x_2(t) \end{pmatrix} + \begin{pmatrix} 0 \\ 1 \end{pmatrix} u(t) \\ y = (10) \begin{pmatrix} x_1(t) \\ x_2(t) \end{pmatrix} \end{cases} \tag{19}$$

i.e.:

$$\begin{cases} \dot{X} = AX + BU \\ Y = CX \end{cases}; A = \begin{pmatrix} 0 & 1 \\ -\frac{K'}{RJ} & -\frac{k^2}{RJ} \end{pmatrix}; B = \begin{pmatrix} 0 \\ 1 \end{pmatrix}; C = \begin{pmatrix} 1 & 0 \end{pmatrix} \tag{20}$$

Given:

$$a_0 = -\frac{K'}{RJ}; a_1 = -\frac{k^2}{RJ}$$

Figure 10 shows the state representation of our system:

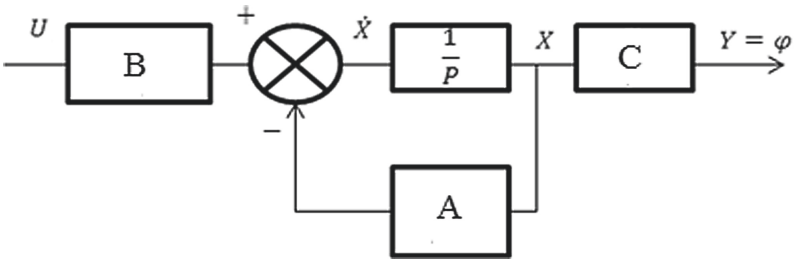

Fig. 10. Representation of the state of the system from its transfer function in LF, considering the angle φ as output from the system.

7 System Control

The sliding mode control (SMC) is a discontinuous and non-linear control technique, it belongs to the family of variable structure controls. SMCs are known for their robustness in the face of disturbances, modelling errors and parametric uncertainties.

The sliding surface is a function which represents the variation over time of the states of the system. The cancellation of the latter corresponds to the cancellation of the magnitude of state considered and the state of stability of the system.

The sliding surface denoted S is given in the following relation:

$$S = \dot{X} + \tau X \tag{20}$$

When the sliding surface S cancels this ensures that the state variable tends towards 0 in a finite time, therefore the stability of the system is guaranteed as long as S = 0.

By setting X = e, with e: error of the system it is therefore possible to ensure the convergence of the error towards 0, consequently the system will respond in finite time and with an error tending towards 0 to a bounded input. For this reason, it is appropriate to choose e = X.

7.1 Stability in the Sense of Lyapunov

Let be the Lyapunov function V(S), in order to ensure the asymptotic stability of the solution of the equation S(x) = 0, it is necessary and sufficient that:

$$V(S) > 0; V(0) = 0; \dot{V}(S) < 0; \dot{V}(0) = 0 \tag{21}$$

If the Lyapunov function satisfies the conditions cited, then the solutions of the equation S(x) = 0 is asymptotically stable.

By putting

$$S = Ge, G = (\gamma + 1), avec\, \gamma > 0 \tag{22}$$

Where e is the error

$$if\ S = 0;\ then\ e = 0$$

The Eq. (22) ensures the convergence of the system error towards a zero value guaranteeing the stability as well as the precision of the latter.

Let Lyapunov's function:

$$V(S) = \frac{S^2}{2} \tag{23}$$

$$\dot{V}(S) = S\dot{S} \tag{24}$$

Let's put:

$$\dot{V}(S) = -S^2 \tag{25}$$

From previous equations we get:

$$-S^2 = \dot{S}S \rightarrow S\left(\dot{S} + S\right) = 0 \tag{26}$$

From other part

$$S = G.e = \left(\gamma\ 1\right).(X_d - X), ou\ X = \begin{pmatrix} x_1 \\ x_2 \end{pmatrix} \tag{27}$$

$$\dot{S} = G\left(\dot{X}_d - \dot{X}\right) \tag{28}$$

From Eq. (26)

$$G\left(\dot{X}_d - \dot{X}\right) = -S \tag{29}$$

Hence

$$GX_d - GAX - GBu_c = -S$$

$$u_c = (S - GAX + GAX_d)(GB)^{-1} \tag{30}$$

$V(S)$, $\dot{V}(S)$ both satisfy Lyapunov's stability criteria, by applying the command u_c to our system, we will obtain that the latter is maintained on the hyperplane S = 0, canceling the error and ensuring in fact stability is the convergence of the system.

7.2 Control Law

u_c, is the command to be applied to the system in order to ensure that the latter is in sliding mode where S = 0, thus ensuring the cancellation of the system error in a finite time (stability and precision).

As shown in (16), $x_1(t)$ physically represents the output of the system (the angle φ), $x_2(t)$ represents the angular speed of the system $\dot{\varphi}$, constant as stipulated in the specifications, $x_2(t)$ is therefore the angular acceleration of the system is worth 0. We will then have:

$$X_d = \begin{pmatrix} \varphi_d \\ \dot{\varphi} \end{pmatrix}; \dot{X}_d = \begin{pmatrix} \dot{\varphi} \\ 0 \end{pmatrix} = \dot{X} = \dot{\varphi} \tag{31}$$

The calculation of the u_c, command requires the evaluation of S, which is carried out from the relation in (27). From (27) and from (31) we simplify (30), in fact:

$$S = \begin{pmatrix} \gamma & 1 \end{pmatrix} \begin{pmatrix} \varphi_d - \varphi \\ 0 \end{pmatrix} = \gamma(\varphi_d - \varphi)$$

By replacing in (30)

$$u_c = \left[\gamma w_{mot} - \varphi a_0 - \dot{\varphi}(a_1 + \gamma) + \gamma(\varphi_d - \varphi)\right]$$

$$u_c = \left[\dot{\varphi} a_1 - \varphi(a_0 + \gamma) + \gamma \varphi_d)\right] \tag{32}$$

It is important to remember that the system works as follows:

While the EMG interface provides an input, the setpoint generator increments φ_d by 4.5° (one step), the system must therefore cause φ to reach φ_d the Fig. 11 below shows the system control diagram.

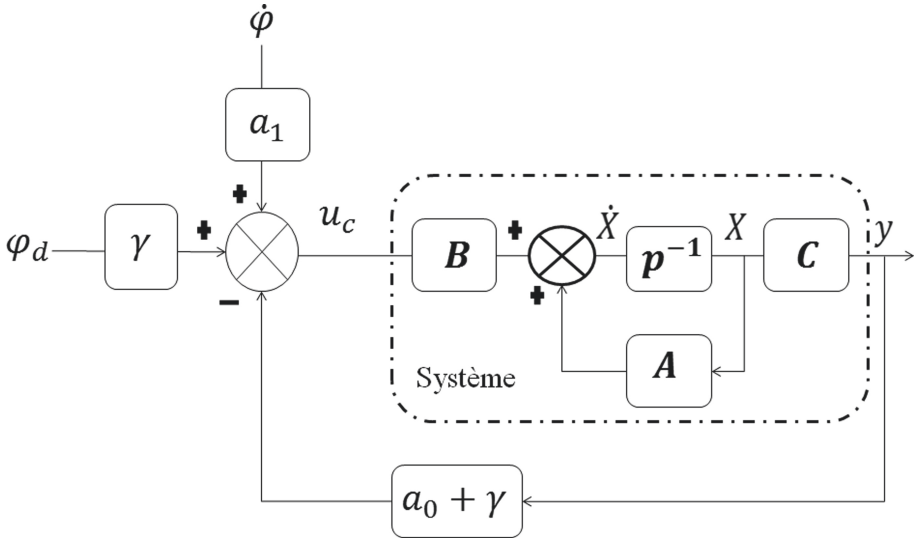

Fig. 11. System control diagram, the SMC controller generates the u_c command necessary to maintain the system in sliding mode from the setpoint φ_d the output φ, parameters a_0, a_1, and the speed $\dot{\varphi} = w_{mot}$ of the number γ.

The controller by sliding mode ensures the stability of the system considered, by choosing a sliding mode (a hyperplane) considering the system error e, the controller also ensures that e converges to a zero value. The SMC overcomes certain constraints, particularly those related to the variation over time of the parameters of the function modelling the system, modelling uncertainties as well as non-linearity.

8 Conclusion

The system presented is a system which can be divided into 2 main parts, the first concerns the determination of the user's intention via the EMG interface, as well as the consequent stimulation of the interactions of the mechatronic structure with its environment. The second part concerns the implementation of the user's intentions through the animation of the mechatronic system (prosthesis), during this the system must reach a position setpoint determined in the upstream part and this by ensuring the convergence of the system error towards a zero value in a finite time.

The control of the system consists in controlling the angle of flexion/extension (φ) of each finger of the prosthesis (independent) via the control of the angle of rotation (θ) delivered by the actuator, knowing the relation $\varphi = f(\theta)$. The block diagrams and the transfer functions illustrate the system and its operation, the angle of rotation of the motor is measured by an angular position sensor materialized by a rotary potentiometer, operated in a conditioning circuit so that the angle of rotation corresponds to a precise tension. The calculation of transfer functions can be subject to modelling uncertainties, as well as to parametric variations, in fact as explained above, certain parameters of the system can evolve or deteriorate over time, such as the value of resistances, the parameters of the engine, the friction of the finger joints, influencing the relation $\varphi = f(\theta)$ in an unpredictable way. For this, our choice fell on a control law which is robust to the constraints mentioned above.

In order to meet the constraints mentioned above, it is necessary to use a control architecture with a variable structure, namely a control law which is not sensitive to variations and to the non-linearity of the model. Several approaches can be envisaged in this context, nevertheless, our approach exploits the SMC, because this approach is relatively simple to implement and it brings satisfactory results in terms of stability and robustness of the system, the SMC was implemented in our approach so as to also ensure the accuracy of the system.

The main drawback when implementing control by sliding mode is what is called chattering, chattering is a vibrational phenomenon due to the switching of the u_c command according to the sign of the S function. indeed, in order to maintain the system in sliding mode ($S = 0$) it is necessary that the command compensates S in order to reduce its value to 0, if $S = K_S$ then u_c must make S vary from $-K_S$ in the case where $S > 0$ and of $+K_S$ in the contrary case, this phenomenon this manifest when the response time of the controller is greater than the response time of the controlled system, in fact, if the command u_c is not dosed correctly by the controller, S may exceed or not reach the hyperplane given the response time of the controller, the system output may reach relatively high values before the controller reacts, this is all the more true if the magnitude of a disturbance we are large where the significant modelling uncertainty.

The command proposed for our system takes into account (as evolving parameters) only the system setpoint as well as its output, relation (32) shows that the u_c command is generated as soon as the setpoint is present and the system responds ($y \neq 0$), there is therefore no delay generated in the response of the controller, thus avoiding the occurrence of chattering at significant amplitude, whatever the amplitude of the disturbances and the uncertainties on the model.

The correction solution provided is a good compromise between the simplicity of implementation and the robustness of the system, indeed, the corrector is simple to implement while guaranteeing the stability and the precision of the system.

References

1. Zhang, T., Ge, S.S., Hang, C.C.: Adaptive neural network control for strict-feedback nonlinear systems using backstepping design. Automatica **36**(12), 1835–1846 (2000)
2. Patre, P.M., Mackunis, W., Kaiser, K., et al.: Asymptotic tracking for uncertain dynamic systems via a multilayer neural network feedforward and RISE feedback control structure. IEEE Trans. Autom. Control **53**(9), 2180–2185 (2008)
3. Liu, Y.-J., Zeng, Q., Tong, S., et al.: Adaptive neural network control for active suspension systems with time-varying vertical displacement and speed constraints. IEEE Trans. Ind. Electron. **66**(12), 9458–9466 (2019)
4. Na, J., Wang, S., Liu, Y.-J., et al.: Finite-time convergence adaptive neural network control for nonlinear servo systems. IEEE Trans. Cybern. **50**(6), 2568–2579 (2019)
5. Shi, X., Cheng, Y., Yin, C., et al.: Design of adaptive backstepping dynamic surface control method with RBF neural network for uncertain nonlinear system. Neurocomputing **330**, 490–503 (2019)
6. Luan, F., Na, J., Huang, Y., et al.: Adaptive neural network control for robotic manipulators with guaranteed finite-time convergence. Neurocomputing **337**, 153–164 (2019)
7. Jia, C., Li, X., Wang, K., et al.: Adaptive control of nonlinear system using online error minimum neural networks. ISA Trans. **65**, 125–132 (2016)
8. Hayakawa, T., Haddad, W.M., Hovakimyan, N.: Neural network adaptive control for nonlinear uncertain dynamical systems with asymptotic stability guarantees. In: Proceedings of the 2005, American Control Conference, 2005, pp. 1301–1306. IEEE (2005)
9. Nguyen, A.-T., Taniguchi, T., Eciolaza, L., et al.: Fuzzy control systems: past, present and future. IEEE Comput. Intell. Mag. **14**(1), 56–68 (2019)
10. Zhang, Z., Liang, H., Wu, C., et al.: Adaptive event-triggered output feedback fuzzy control for nonlinear networked systems with packet dropouts and actuator failure. IEEE Trans. Fuzzy Syst. **27**(9), 1793–1806 (2019)
11. Qiu, J., Sun, K., Wang, T., et al.: Observer-based fuzzy adaptive event-triggered control for pure-feedback nonlinear systems with prescribed performance. IEEE Trans. Fuzzy Syst. **27**(11), 2152–2162 (2019)
12. Škrjanc, I., Iglesias, J.A., Sanchis, A., et al.: Evolving fuzzy and neuro-fuzzy approaches in clustering, regression, identification, and classification: a survey. Inf. Sci. **490**, 344–368 (2019)
13. Zahedi, F., Zahedi, Z.: A review of neuro-fuzzy systems based on intelligent control. arXiv preprint arXiv:1805.03138 (2018)
14. Khosravi, A., Koury, R.N.N., Machado, L., et al.: Prediction of wind speed and wind direction using artificial neural network, support vector regression and adaptive neuro-fuzzy inference system. Sustain. Energy Technol. Assess. **25**, 146–160 (2018)

15. Kamil, A., Rustamov, S., Clement, M., Mustafayev, E.: Adaptive neuro-fuzzy inference system for classification of texts. In: Zadeh, L.A., Yager, R.R., Shahbazova, S.N., Reformat, M.Z., Kreinovich, V. (eds.) Recent Developments and the New Direction in Soft-Computing Foundations and Applications. SFSC, vol. 361, pp. 63–70. Springer, Cham (2018). https://doi.org/10.1007/978-3-319-75408-6_6
16. Shihabudheen, K.V., Pillai, G.N.: Recent advances in neuro-fuzzy system: a survey. Knowl. Based Syst. **152**, 136–162 (2018)
17. Li, H., Shi, P., Yao, D., et al.: Observer-based adaptive sliding mode control for nonlinear Markovian jump systems. Automatica **64**, 133–142 (2016)
18. Plestan, F., Shtessel, Y., Bregeault, V., et al.: New methodologies for adaptive sliding mode control. Int. J. Control **83**(9), 1907–1919 (2010)
19. Ferrara, A., Incremona, G.P.: Design of an integral suboptimal second-order sliding mode controller for the robust motion control of robot manipulators. IEEE Trans. Control Syst. Technol. **23**(6), 2316–2325 (2015)
20. Huber, O., Acary, V., Brogliato, B.: Lyapunov stability and performance analysis of the implicit discrete sliding mode control. IEEE Trans. Autom. Control **61**(10), 3016–3030 (2015)
21. Huber, O., Brogliato, B., Acary, V., et al.: Experimental results on implicit and explicit time-discretization of equivalent-control-based sliding-mode control (2016)
22. Slotine, J.-J.E., Li, W., et al.: Applied Nonlinear Control. Prentice Hall, Englewood Cliffs (1991)
23. Utkin, V., Guldner, J., Shi, J.: Sliding Mode Control in Electro-Mechanical Systems. CRC Press, Boca Raton (2009)
24. Boiko, I., Fridman, L.: Analysis of chattering in continuous sliding-mode controllers. IEEE Trans. Autom. Control **50**(9), 1442–1446 (2005)
25. Boiko, I., Fridman, L., Pisano, A., et al.: Performance analysis of second-order sliding-mode control systems with fast actuators. IEEE Trans. Autom. Control **52**(6), 1053–1059 (2007)
26. Choi, S.-B., Park, D.-W., Jayasuriya, S.: A time-varying sliding surface for fast and robust tracking control of second-order uncertain systems. Automatica **30**(5), 899–904 (1994)
27. Levant, A.: Sliding order and sliding accuracy in sliding mode control. Int. J. Control **58**(6), 1247–1263 (1993)
28. Bartolini, G., Ferrara, A., Usai, E., et al.: On multi-input chattering-free second-order sliding mode control. IEEE Trans. Autom. Control **45**(9), 1711–1717 (2000)
29. Laghrouche, S., Plestan, F., Glumineau, A.: Higher order sliding mode control based on integral sliding mode. Automatica **43**(3), 531–537 (2007)
30. Plestan, F., Glumineau, A., Laghrouche, S.: A new algorithm for high-order sliding mode control. Int. J. Robust Nonlinear Control: IFAC-Affiliated J. **18**(4–5), 441–453 (2008)
31. Benchabane, S.I., Saadia, N., Ramdane-Cherif, A.: Novel algorithm for conventional myocontrol of upper limbs prosthetics. Biomed. Signal Process. Control **57**, 101791 (2020)